

Neutron-rich hypernuclei: ${}^6_{\Lambda}\text{H}$ and beyond

A. Gal^{a,*}, D.J. Millener^b

^a*Racah Institute of Physics, The Hebrew University, 91904 Jerusalem, Israel*

^b*Physics Department, Brookhaven National Laboratory, Upton, NY 11973, USA*

Abstract

Recent experimental evidence presented by the FINUDA Collaboration for a particle-stable ${}^6_{\Lambda}\text{H}$ has stirred renewed interest in charting domains of particle-stable neutron-rich Λ hypernuclei, particularly for unbound nuclear cores. We have studied within a shell-model approach several neutron-rich Λ hypernuclei in the nuclear p shell that could be formed in (π^-, K^+) or in (K^-, π^+) reactions on stable nuclear targets. Hypernuclear shell-model input is taken from a theoretically inspired successful fit of γ -ray transitions in p -shell Λ hypernuclei which includes also $\Lambda N \leftrightarrow \Sigma N$ coupling ($\Lambda\Sigma$ coupling). The particle stability of ${}^6_{\Lambda}\text{H}$ is discussed and predictions are made for binding energies of ${}^9_{\Lambda}\text{He}$, ${}^{10}_{\Lambda}\text{Li}$, ${}^{12}_{\Lambda}\text{Be}$, ${}^{14}_{\Lambda}\text{B}$. None of the large effects conjectured by some authors to arise from $\Lambda\Sigma$ coupling is borne out, neither by these realistic p -shell calculations, nor by quantitative estimates outlined for heavier hypernuclei with substantial neutron excess.

Keywords:

hypernuclei, effective interactions in hadronic systems, shell model

PACS: 21.80.+a, 21.30.Fe, 21.60.Cs

1. Introduction

Dalitz and Levi Setti, fifty years ago [1], discussed the possibility that Λ hyperons could stabilize particle-unstable nuclear cores of Λ hypernuclei and thus allow studies of neutron-rich baryonic systems beyond the nuclear drip line. The Λ 's effectiveness to enhance binding is primarily connected with the Pauli principle from which it is exempt, allowing it to occupy the lowest

*Corresponding author: Avraham Gal, avragal@vms.huji.ac.il

$0s_\Lambda$ orbital. Several unbound-core Λ hypernuclei have since been identified in emulsion work, the neutron richest of which is ${}^8_\Lambda\text{He}$ [2]. Of particular interest is the recent FINUDA evidence for a particle-stable ${}^6_\Lambda\text{H}$ hypernucleus produced in the ${}^6\text{Li}(K^-_{\text{stop}}, \pi^+)$ reaction [3, 4]. In distinction from the well-established hyper-hydrogen isotopes ${}^{3,4}_\Lambda\text{H}$, the ${}^5\text{H}$ nuclear core of ${}^6_\Lambda\text{H}$ is unbound, and its neutron-proton excess ratio $(N - Z)/(N + Z) = 0.6$ is unsurpassed by any stable or Λ -stabilized core nucleus. The ${}^6_\Lambda\text{H}$ hypernucleus was highlighted in Ref. [5] as a testground for the significance of $\Lambda\Sigma$ coupling in Λ hypernuclei, spurred by the role it plays in s -shell hypernuclei [6, 7] and by the far-reaching consequences it might have for dense neutron-star matter with strangeness [8]. In the present work, and as a prelude to its main theme, we discuss the particle stability of ${}^6_\Lambda\text{H}$ from the point of view of the shell model, focusing on $\Lambda\Sigma$ coupling contributions and making comparisons with other calculations and with the FINUDA experimental evidence.

The purpose of this Letter is to provide shell-model predictions for other neutron-rich Λ hypernuclei that could be reached at J-PARC in (π^-, K^+) or (K^-, π^+) reactions on stable nuclear targets in the p shell. A missing-mass ${}^6\text{Li}(\pi^-, K^+)$ spectrum from J-PARC in-flight experiment E10 [9] is under study at present, aimed at assessing independently FINUDA's evidence for a particle-stable ${}^6_\Lambda\text{H}$ hypernucleus. In the present analysis, based on extensive hypernuclear shell-model calculations [10], we use $0p_N 0s_\Lambda$ effective interactions with matrix elements constrained by the most comprehensive set of hypernuclear γ -ray measurements [11]. Included explicitly are also $0p_N 0s_\Lambda \leftrightarrow 0p_N 0s_\Sigma$ effective interactions based on the $0s_N 0s_Y$ G -matrix interactions ($Y = \Lambda, \Sigma$) used in the comprehensive s -shell hypernuclear calculations of Ref. [6]. The methodology of this shell-model analysis is briefly reviewed in Section 2, following which we discuss ${}^6_\Lambda\text{H}$ in Section 3 and then, in Section 4, the neutron-rich hypernuclei that can be produced on stable nuclear targets in the nuclear p shell. Predictions are made for the corresponding ground-state binding energies. Also outlined in this section is a shell-model evaluation of $\Lambda\Sigma$ coupling effects in heavier hypernuclei with larger neutron excess, such as ${}^{49}_\Lambda\text{Ca}$ and ${}^{209}_\Lambda\text{Pb}$, demonstrating that the increase in neutron excess is more than compensated by the decrease of the $\Lambda\Sigma$ coupling matrix elements with increasing orbital angular momentum ℓ_N of the valent nucleon configurations involved in the coherent coupling approximation. We thus conclude that none of the large effects conjectured in Ref. [5] to arise from $\Lambda\Sigma$ coupling is borne out in realistic calculations.

2. Shell-model methodology

The ΛN effective interaction

$$V_{\Lambda N} = \bar{V} + \Delta \vec{s}_N \cdot \vec{s}_\Lambda + \mathcal{S}_\Lambda \vec{l}_N \cdot \vec{s}_\Lambda + \mathcal{S}_N \vec{l}_N \cdot \vec{s}_N + \mathcal{T} S_{N\Lambda}, \quad (1)$$

where $S_{N\Lambda} = 3(\vec{\sigma}_N \cdot \vec{r})(\vec{\sigma}_\Lambda \cdot \vec{r}) - \vec{\sigma}_N \cdot \vec{\sigma}_\Lambda$, is specified here by its $0p_N 0s_\Lambda$ spin-dependent matrix elements within a $0\hbar\omega$ shell-model space [12]. The same parametrization applies also to the $\Lambda\Sigma$ coupling interaction and the ΣN interaction for both isospin 1/2 and 3/2, with an obvious generalization to account for the isospin 1 of the Σ hyperon [10]. The detailed properties of the ΣN interaction parameters hardly matter in view of the large energy denominators of order $M_\Sigma - M_\Lambda \approx 80$ MeV with which they appear. To understand the effects of the $\Lambda\Sigma$ coupling interaction, it is convenient to introduce an overall isospin factor $\sqrt{4/3} \vec{t}_N \cdot \vec{t}_{\Lambda\Sigma}$, where $\vec{t}_{\Lambda\Sigma}$ converts a Λ to Σ in isospace. Matrix elements of the ΛN effective interaction (1) and of the $\Lambda\Sigma$ coupling interaction are listed in Table 1. The ΛN matrix elements were fitted to a wealth of hypernuclear γ -ray measurements [13], resulting in values close to those derived from the YN interaction models NSC97 [14]. The $\Lambda\Sigma$ matrix elements are derived from the same NSC97 models used to construct $0s_N 0s_Y$ G -matrix interactions in s -shell Λ hypernuclear calculations [6]. By limiting here the ΣN model-space to $0p_N 0s_\Sigma$, in parallel to the $0\hbar\omega$ $0p_N 0s_\Lambda$ model-space used for ΛN , we maintain the spirit of Akaishi's *coherent* approximation [5, 6] which is designed to pick up the strongest $\Lambda\Sigma$ matrix elements.¹

It is clear from Table 1 that the only significant $\Lambda\Sigma$ interaction parameters are $\bar{V}_{\Lambda\Sigma}$ and $\Delta_{\Lambda\Sigma}$, in obvious notation. The first one is associated with diagonal matrix elements of the spin-independent part of the $\Lambda\Sigma$ interaction, viz.

$$\langle (J_N T, s_\Lambda) JT | V_{\Lambda\Sigma} | (J_N T, s_\Sigma) JT \rangle = \sqrt{4/3} \sqrt{T(T+1)} \bar{V}_{\Lambda\Sigma}. \quad (2)$$

This part preserves the nuclear core, specified here by its total angular momentum J_N and isospin T , with matrix elements that bear resemblance to

¹By *coherent* we mean $nl_N 0s_\Lambda \leftrightarrow nl_N 0s_\Sigma$ coupling that preserves hyperon and nucleon orbits, where nl_N denotes the nuclear orbits occupied in the core-nucleus wavefunction. For the $A = 4$ hypernuclei considered by Akaishi et al. [6], this definition reduces to the assumption that the Λ and Σ , both in their $0s$ orbits, are coupled to the *same* nuclear core state. The parameters listed in the last line of Table 1 contribute almost 0.6 MeV to the binding of ${}^4_\Lambda\text{H}(0_{g.s.}^+)$ and more than 0.5 MeV to the excitation energy of ${}^4_\Lambda\text{H}(1_{\text{exc.}}^+)$.

Table 1: $0l_N0s_\Lambda \leftrightarrow 0l_N0s_Y$ matrix elements (in MeV) from Ref. [10]. \bar{V} and Δ are the spin-average and difference of the triplet and singlet central matrix elements. For the $s^3_{N s_Y}$ hypernuclei, the $\Lambda\Sigma$ coupling matrix elements are $v(0^+_{g.s.}) = \bar{V}_{\Lambda\Sigma}^{0s} + \frac{3}{4}\Delta_{\Lambda\Sigma}^{0s}$ and $v(1^+_{exc.}) = \bar{V}_{\Lambda\Sigma}^{0s} - \frac{1}{4}\Delta_{\Lambda\Sigma}^{0s}$, with downward energy shifts $\delta E_{\downarrow}(J^\pi) \approx v^2(J^\pi)/(80 \text{ MeV})$.

Y	$0l_N$	\bar{V}	Δ	\mathcal{S}_Λ	\mathcal{S}_N	\mathcal{T}
$\Lambda (A \leq 9)$	$0p_N$		0.430	-0.015	-0.390	0.030
$\Lambda (A \geq 10)$	$0p_N$		0.330	-0.015	-0.350	0.024
Σ	$0p_N$	1.45	3.04	-0.09	-0.09	0.16
Σ	$0s_N$	2.96	5.09	-	-	-

the Fermi matrix elements in β decay of the core nucleus. Similarly, the spin-spin part of the $\Lambda\Sigma$ interaction associated with the matrix element $\Delta_{\Lambda\Sigma}$ involves the operator $\sum_j \vec{s}_{Nj} \vec{t}_{Nj}$ for the core, connecting core states with large Gamow-Teller (GT) transition matrix elements as emphasized recently by Umeya and Harada in their study of the ${}^7\text{-}^{10}\text{Li}$ isotopes [15].

Finally, the ΛN spin-independent matrix element \bar{V} is not specified in Table 1 because it is not determined by fitting hypernuclear γ -ray transitions. Its value is to be deduced from fitting absolute binding energies. Suffice to say that \bar{V} assumes values of $\bar{V} \approx -1.0 \pm 0.1$ MeV [10]. We consider it as part of a mean-field description of Λ hypernuclei, consistent with the observation that on the average throughout the p shell $B_\Lambda(A)$ increases by about 1 MeV upon increasing A by one unit, with a 0.1 MeV uncertainty that might reflect genuine YNN three-body contributions [16, 17].

3. ${}^6_\Lambda\text{H}$

The low-lying spectrum of ${}^6_\Lambda\text{H}$ consists of a $0^+_{g.s.}$ and $1^+_{exc.}$ states which, disregarding the two p -shell neutrons known from ${}^6\text{He}$ to couple dominantly to $L = S = 0$, are split in ${}^4_\Lambda\text{H}$ by 1.08 ± 0.02 MeV [18]. These states in ${}^6_\Lambda\text{H}$ are split by 1.0 ± 0.7 MeV, judging by the systematic difference noted in the FINUDA experiment [3, 4] between the mass values $M({}^6_\Lambda\text{H})$ from production and decay, as shown in Fig. 1. The observation of ${}^6_\Lambda\text{H} \rightarrow \pi^- + {}^6\text{He}$ weak decay in the FINUDA experiment implies that ${}^6_\Lambda\text{H}$ is particle-stable, with $2n$ separation energy $B_{2n}({}^6_\Lambda\text{H}_{g.s.}) = 0.8 \pm 1.2$ MeV, independently of the location of the core-nucleus ${}^5\text{H}$ resonance.

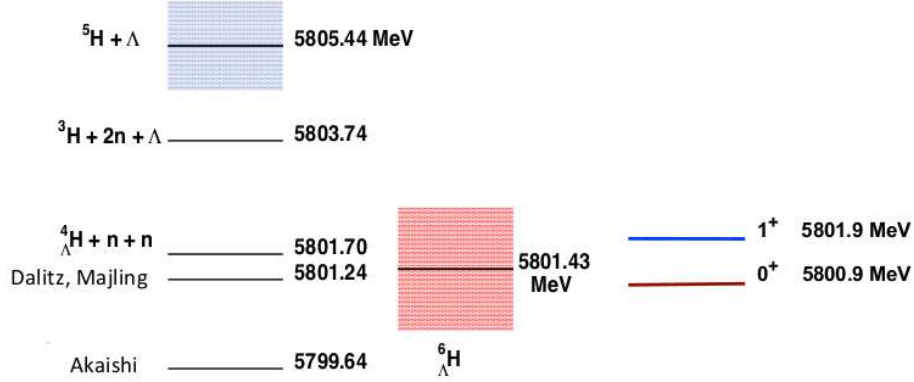


Figure 1: ${}^6_{\Lambda}\text{H}$ binding energy diagram adapted from Ref. [4], with thresholds marked on its upper-left side and theory predictions beneath [1, 19]. The location of the ${}^5\text{H}$ resonance vs. the ${}^3\text{H}+2n$ threshold, with the (blue) hatched box denoting its width, is taken from Ref. [20]. The (red) shaded box represents the error on the mean production and decay mass value obtained from the three FINUDA events assigned to ${}^6_{\Lambda}\text{H}$, whereas the positions of the $1^+_{\text{exc.}}$ and $0^+_{\text{g.s.}}$ levels marked on the right-hand side are derived separately from production and decay, respectively. We thank Elena Botta for providing this figure.

3.1. Phenomenological shell-model analysis

A phenomenological shell-model estimate for $B_{\Lambda}({}^6_{\Lambda}\text{H})$ cited in Ref. [4], also bypassing ${}^5\text{H}$, yields

$$B_{\Lambda}({}^6_{\Lambda}\text{H}) = B_{\Lambda}({}^4_{\Lambda}\text{H}) + [B_{\Lambda}({}^7_{\Lambda}\text{He}) - B_{\Lambda}({}^5_{\Lambda}\text{He})] = (2.04 \pm 0.04) + (2.24 \pm 0.09) \text{ MeV}, \quad (3)$$

based on the value $B_{\Lambda}({}^7_{\Lambda}\text{He}) = (5.36 \pm 0.09) \text{ MeV}$ obtained by extrapolating linearly the known binding energies of the other $T = 1$ isotriplet members of the $A = 7$ hypernuclei.² The argument underlying this derivation is that the total Λnn interaction, including $\Lambda\Sigma$ coupling contributions, is given by the difference of Λ binding energies within the square bracket, assuming that the Λnn configuration for the two p -shell neutrons in ${}^6_{\Lambda}\text{H}$ is identical with that in ${}^7_{\Lambda}\text{He}$. Accepting then the ${}^5\text{H}$ mass determination from Ref. [20] one obtains

²The value $B_{\Lambda}({}^7_{\Lambda}\text{He}) = 5.68 \pm 0.03(\text{stat.}) \pm 0.22(\text{syst.}) \text{ MeV}$, obtained recently from Jlab E01-011 [21], is irreproducible also in related few-body cluster calculations [22].

the corresponding phenomenological shell-model estimate for $B_{2n}({}^6_{\Lambda}\text{H})$:

$$B_{2n}({}^6_{\Lambda}\text{H}) = B_{2n}({}^5\text{H}) + [B_{\Lambda}({}^6_{\Lambda}\text{H}) - B_{\Lambda}({}^4_{\Lambda}\text{H})] = (-1.7 \pm 0.3) + (2.24 \pm 0.09) \text{ MeV}, \quad (4)$$

yielding $B_{2n}({}^6_{\Lambda}\text{H}) = (0.5 \pm 0.3) \text{ MeV}$ which, however, is not independent of the resonance location of ${}^5\text{H}$. Equation (4) demonstrates the gain in *nuclear* binding owing to the added Λ hyperon.

3.2. Refined shell-model analysis

The phenomenological shell-model estimate outlined above needs to be refined on two counts as follows. First, one notes that the nuclear s shell is not closed in ${}^6_{\Lambda}\text{H}$, in distinction from all other neutron-rich Λ hypernuclei considered in the present work, so that the $\Lambda\Sigma$ coupling contribution in ${}^6_{\Lambda}\text{H}$ is not the sum of the separate contributions from the s shell through ${}^4_{\Lambda}\text{H}$ and from the p shell through ${}^7_{\Lambda}\text{He}$. For an s^3p^2 core of ${}^6_{\Lambda}\text{H}$, with [32] spatial symmetry and $T=3/2$, the coherent $\Lambda\Sigma$ coupling diagonal matrix element is $\sqrt{5/9}v(J^\pi) + \sqrt{20/9}\bar{V}_{\Lambda\Sigma}^{0p}$ for $J^\pi = 0^+, 1^+$, where $v(J^\pi)$ is the corresponding $A=4$ matrix element (see caption to Table 1), with no contribution from $\Delta_{\Lambda\Sigma}^{0p}$ because the two p -shell neutrons have Pauli spin zero. $\Lambda\Sigma$ contributions to the binding energies of Λ hypernuclei involved in the shell-model evaluation of the ${}^6_{\Lambda}\text{H}$ doublet levels $0_{\text{g.s.}}^+$ and $1_{\text{exc.}}^+$, calculated for the interaction specified in Table 1, are listed in Table 2.

Table 2: $\Lambda\Sigma$ contributions (in keV) to binding energies of Λ hypernuclei involved in shell-model considerations of ${}^6_{\Lambda}\text{H}$ stability.

J^π	${}^4_{\Lambda}\text{H}$ diag.=tot.	${}^7_{\Lambda}\text{He}(\frac{1}{2}_{\text{g.s.}}^+)$ diag.	${}^7_{\Lambda}\text{He}(\frac{1}{2}_{\text{g.s.}}^+)$ total	${}^6_{\Lambda}\text{H}$ diag.	${}^6_{\Lambda}\text{H}$ total
0^+	574	70	98	650	821
1^+	36	70	98	146	176

Whereas ${}^4_{\Lambda}\text{H}$ admits only a diagonal matrix-element contribution, the p -shell hypernuclei admit both diagonal as well as nondiagonal matrix-element contributions, with the listed diagonal ones dominating. It is also seen that ${}^6_{\Lambda}\text{H}(0_{\text{g.s.}}^+)$ gains 149 keV and ${}^6_{\Lambda}\text{H}(1_{\text{exc.}}^+)$ gains 42 keV binding above the sum of separate contributions from ${}^4_{\Lambda}\text{H}$ and ${}^7_{\Lambda}\text{He}$ inherent in the phenomenological shell-model approach. With respect to ${}^4_{\Lambda}\text{H}$ alone, the $\Lambda\Sigma$ contribution gain

is 247 keV for ${}^6_{\Lambda}\text{H}(0^+_{\text{g.s.}})$ and 140 keV for ${}^6_{\Lambda}\text{H}(1^+_{\text{exc.}})$. Thus, the shell-model predicts a doublet spacing $\Delta E(1^+_{\text{exc.}}-0^+_{\text{g.s.}})$ in ${}^6_{\Lambda}\text{H}$ of only 0.1 MeV larger than in ${}^4_{\Lambda}\text{H}$ owing to the $\Lambda\Sigma$ coupling, considerably less than the additional 1.4 MeV argued by Akaishi et al. [5, 19].

A more important reason for revising the phenomenological shell-model estimate is the reduction of matrix elements that involve spatially extended p -shell neutrons in ${}^6_{\Lambda}\text{H}$ ($B_{2n} \lesssim 0.8$ MeV) relative to matrix elements that involve a more compact p -shell neutron in ${}^7_{\Lambda}\text{He}$ ($B_n \sim 3.0$ MeV). The average neutron separation energy in ${}^6_{\Lambda}\text{H}$ is closer to that in ${}^6_{\Lambda}\text{He}$ ($B_n = 0.26 \pm 0.10$ MeV). Using our shell-model estimates for the spin-dependent and $\Lambda\Sigma$ coupling contributions to $B_{\Lambda}({}^6_{\Lambda}\text{He})$, we deduce $\bar{V} \sim -0.8$ MeV and a similar 20% reduction in other $0p_N 0s_{\Lambda}$ interaction matrix elements, thereby yielding

$$B_{\Lambda}({}^6_{\Lambda}\text{H}) \sim B_{\Lambda}({}^4_{\Lambda}\text{H}) + 0.8[B_{\Lambda}({}^7_{\Lambda}\text{He}) - B_{\Lambda}({}^5_{\Lambda}\text{He})] = (3.83 \pm 0.08 \pm 0.22) \text{ MeV}, \quad (5)$$

where the first uncertainty is due to the statistical uncertainty of the binding-energy input [2] and the second, systematic uncertainty assumes that the 0.8 renormalization factor is uncertain to within 0.1. Accepting, again, the ${}^5\text{H}$ resonance location from [20], a revised estimate follows: $B_{2n}({}^6_{\Lambda}\text{H}) \approx (0.1 \pm 0.4)$ MeV. Because the s^3p^2 core for ${}^6_{\Lambda}\text{H}$ will be more spatially extended than the α -particle core for the He hypernuclei, a few-body calculation such as that of Hiyama et al. [23], discussed below, is required.³ We therefore consider the present revised shell-model estimate, listed also in Table 3 below, as an upper bound for $B_{\Lambda}({}^6_{\Lambda}\text{H})$.

In Table 3 we compare several theoretical ${}^6_{\Lambda}\text{H}$ predictions to each other and to FINUDA's findings. The table makes it clear that FINUDA's results do not support the predictions made in Refs. [5, 19] according to which the two p -shell neutrons in ${}^6_{\Lambda}\text{H}$ enhance the $\Lambda\Sigma$ coupling contribution in ${}^4_{\Lambda}\text{H}$, thereby pushing down the ${}^6_{\Lambda}\text{H}(0^+_{\text{g.s.}})$ level by twice as much as it does in ${}^4_{\Lambda}\text{H}$ and thus doubling the $0^+_{\text{g.s.}}-1^+_{\text{exc.}}$ spacing. In contrast to such overbound ${}^6_{\Lambda}\text{H}$, the recent ${}^3\text{H}-n-n-\Lambda$ four-body calculation by Hiyama et al. [23] does not bind ${}^6_{\Lambda}\text{H}$. This calculation is the only one that considers dynamically the ${}^5\text{H}$ core as a three-body ${}^3\text{H}-n-n$ resonance, but then it disregards $\Lambda\Sigma$ coupling which is a necessary ingredient in any ${}^6_{\Lambda}\text{H}$ calculation owing to the

³Comparing p -shell neutron densities for a slightly bound ${}^6_{\Lambda}\text{H}$ [23] with those for ${}^7_{\Lambda}\text{He}$ [22] in four-body $\text{C}-n-n-\Lambda$ calculations, where the cluster C stands for ${}^3\text{H}$ or ${}^4\text{He}$ respectively, supports our $\approx 20\%$ reduction of ΛN and $\Lambda\Sigma$ matrix elements in going from ${}^7_{\Lambda}\text{He}$ to ${}^6_{\Lambda}\text{H}$. We thank Emiko Hiyama for providing us with plots of these densities.

Table 3: ${}^6_{\Lambda}\text{H}(0^+_{\text{g.s.}})$ binding energies $B_{2n/\Lambda}$ and doublet spacing $\Delta E(1^+_{\text{exc.}} - 0^+_{\text{g.s.}})$ predictions vs. experiment. E_{2n} marks the assumed ${}^5\text{H}$ resonance position w.r.t. $2n$ emission.

B & ΔE (MeV)	Akaishi		shell model	Hiyama	FINUDA
	[5]	[19]	this work	[23]	exp. [3, 4]
$E_{2n}({}^5\text{H})$	2.1	1.7	1.7 ± 0.3	1.6	–
$B_{2n}({}^6_{\Lambda}\text{H})$	1.7	2.1	0.1 ± 0.4	–1.1	0.8 ± 1.2
$B_{\Lambda}({}^6_{\Lambda}\text{H})$	5.8	5.8	3.8 ± 0.2	2.5	4.5 ± 1.2
$\Delta E({}^6_{\Lambda}\text{H})$	2.4	2.4	1.2 ± 0.1	–	1.0 ± 0.7

lowest particle-stability threshold which involves ${}^4_{\Lambda}\text{H}$. Our own shell-model estimate, allowing approximately for a spatially extended $2n$ cluster, suggests a very weakly bound ${}^6_{\Lambda}\text{H}(0^+_{\text{g.s.}})$ and a particle-unstable ${}^6_{\Lambda}\text{H}(1^+_{\text{exc.}})$ that decays by emitting a low-energy neutron pair:

$${}^6_{\Lambda}\text{H}(1^+_{\text{exc.}}) \rightarrow {}^4_{\Lambda}\text{H}(0^+_{\text{g.s.}}) + 2n. \quad (6)$$

However, this decay is substantially suppressed both kinematically and dynamically, kinematically since s -wave emission requires a 3S_1 dineutron configuration which is Pauli-forbidden, and the allowed p -wave emission which is kinematically suppressed at low energy requires that *both* ${}^6_{\Lambda}\text{H}$ constituents, ${}^4_{\Lambda}\text{H}$ and $2n$, flip their Pauli spin which is disfavored dynamically. This leaves open the possibility that $M1$ γ emission to ${}^6_{\Lambda}\text{H}(0^+_{\text{g.s.}})$ provides a competitive decay mode of the $1^+_{\text{exc.}}$ level.

4. Neutron-rich hypernuclei beyond ${}^6_{\Lambda}\text{H}$

In the first part of this section we consider neutron-rich Λ hypernuclei that can be produced in double-charge exchange reactions (π^-, K^+) or (K^-, π^+) on stable nuclear targets in the p shell. These are ${}^6_{\Lambda}\text{H}$, which was discussed in the previous section, ${}^9_{\Lambda}\text{He}$, ${}^{10}_{\Lambda}\text{Li}$, ${}^{12}_{\Lambda}\text{Be}$, and ${}^{14}_{\Lambda}\text{B}$, with targets ${}^6\text{Li}$, ${}^9\text{Be}$, ${}^{10}\text{B}$, ${}^{12}\text{C}$, and ${}^{14}\text{N}$, respectively.⁴ In distinction from the unbound-core ${}^6_{\Lambda}\text{H}$,

⁴We excluded ${}^{16}_{\Lambda}\text{C}$ which can be produced on ${}^{16}\text{O}$ target because its analysis involves $(1s - 0d)_N 0s_{\Lambda}$ matrix elements which are not constrained by any hypernuclear datum. For the same reason we ignored for ${}^{12}_{\Lambda}\text{Be}$ the positive-parity doublet built on ${}^{11}\text{Be}_{\text{g.s.}}(\frac{1}{2}^+)$, considering only the normal-parity doublet based on the $\frac{1}{2}^-$ excited state at 0.32 MeV.

all other neutron-rich Λ hypernuclei listed above are based on bound nuclear cores, which ensures their particle stability together with that of a few excited states. In the second half of the present section we outline the evaluation of $\Lambda\Sigma$ coupling matrix elements in heavier nuclear cores with substantial neutron excess, ^{48}Ca and ^{208}Pb .

4.1. *p*-shell neutron-rich hypernuclei beyond $^6_\Lambda\text{H}$

Table 4: Beyond-mean-field $\Delta B_\Lambda^{\text{g.s.}}$ shell-model contributions to normal-parity ground states of neutron-rich hypernuclei (in MeV); see text. ME stands for “matrix element”.

target AZ	<i>n</i> -rich $^A_\Lambda(Z-2)$	ME diag.	$\Lambda\Sigma$ diag.	$\Lambda\Sigma$ total	induced $\vec{l}_N \cdot \vec{s}_N$	$\Delta B_\Lambda^{\text{g.s.}}$ total
^9Be	$^9_\Lambda\text{He}(\frac{1}{2}^+)$	4.101	0.210	0.253	0.619	0.879
^{10}B	$^{10}_\Lambda\text{Li}(1^-)$	4.023	0.202	0.275	0.595	1.022
^{12}C	$^{12}_\Lambda\text{Be}(0^-)$	3.835	0.184	0.158	0.554	0.748
^{14}N	$^{14}_\Lambda\text{B}(1^-)$	3.884	0.189	0.255	0.458	0.785

In Table 4, we focus on $\Lambda\Sigma$ contributions to binding energies of normal-parity g.s. in neutron-rich *p*-shell hypernuclei. Column 3 gives the diagonal matrix-element (ME) from the central components $\bar{V}_{\Lambda\Sigma}^{0p}$ and $\Delta_{\Lambda\Sigma}^{0p}$ of the coherent $\Lambda\Sigma$ coupling interaction. The contribution from $\bar{V}_{\Lambda\Sigma}^{0p}$ is given by Eq. (2), saturating this diagonal matrix element in $^9_\Lambda\text{He}$ and dominating it with a value 3.242 MeV in the other cases. Column 4 gives the corresponding downward energy shift $(\text{ME})^2/80$ assuming a constant 80 MeV separation between Λ and Σ states, and column 5 gives the energy shift in the full shell-model calculation, accounting also for the noncentral components of the coherent $\Lambda\Sigma$ coupling interaction and including nondiagonal matrix elements as well. Except for $^{12}_\Lambda\text{Be}$ where the decreased shift in the complete calculation is due to the contribution of the noncentral components to the diagonal matrix element, a very good approximation for the total coherent $\Lambda\Sigma$ coupling contribution is obtained using just the central (Fermi and GT) $\Lambda\Sigma$ coupling interaction. In these cases, the increased energy shift beyond the diagonal contribution arises from Σ core states connected to the Λ core state by GT transitions. The shift gets smaller with increased fragmentation of the GT strength. Finally, we note that the total $\Lambda\Sigma$ contribution listed in column 5 agrees for $^{10}_\Lambda\text{Li}$ with that computed in Ref. [24] using the same YN

shell-model interactions. More recently, these authors discussed $\Lambda\Sigma$ coupling effects on g.s. doublet spacings in ${}^{7-10}_{\Lambda}\text{Li}$ isotopes, obtaining moderate enhancements between 70 to 150 keV [15]. We have reached similar conclusions for all the neutron-rich hypernuclei considered in the present work beyond ${}^6_{\Lambda}\text{H}$.

The total $\Lambda\Sigma$ contribution discussed above is only one component of the total beyond-mean-field (BMF) contribution $\Delta B_{\Lambda}^{\text{g.s.}}$. To obtain the latter, various spin-dependent ΛN contributions generated by $V_{\Lambda N}$ have to be added to the total $\Lambda\Sigma$ contributions listed in column 5 of Table 4. Column 6 lists one such spin-dependent ΛN contribution, arising from the Λ -induced $\vec{l}_N \cdot \vec{s}_N$ nuclear spin-orbit term of Eq. (1). By comparing column 5 with column 6, and both with the total BMF contributions listed in column 7, the last one, it is concluded that the majority of the BMF contributions arise from ΛN spin-dependent terms, dominated by $\vec{l}_N \cdot \vec{s}_N$.

Table 5: Binding energy predictions for neutron-rich p -shell hypernuclei (in MeV).

n -rich ${}^A_{\Lambda}Z$	normal ${}^A_{\Lambda}Z'$	normal $B_{\Lambda}^{\text{g.s.}}$	normal $\Delta B_{\Lambda}^{\text{g.s.}}$	n -rich $\Delta B_{\Lambda}^{\text{g.s.}}$	n -rich $B_{\Lambda}^{\text{g.s.}}$
${}^9_{\Lambda}\text{He}(\frac{1}{2}^+)$	${}^9_{\Lambda}\text{Li}/{}^9_{\Lambda}\text{B}$	8.44 ± 0.10	0.952	0.879	8.37 ± 0.10
${}^{10}_{\Lambda}\text{Li}(1^-)$	${}^{10}_{\Lambda}\text{Be}/{}^{10}_{\Lambda}\text{B}$	8.94 ± 0.11	0.518	1.022	9.44 ± 0.11
${}^{12}_{\Lambda}\text{Be}(0^-)$	${}^{12}_{\Lambda}\text{B}$	11.37 ± 0.06	0.869	0.748	11.25 ± 0.06
${}^{14}_{\Lambda}\text{B}(1^-)$	${}^{14}_{\Lambda}\text{C}$	12.17 ± 0.33	0.904	0.785	12.05 ± 0.33

Our Λ binding energy predictions for ground states of neutron-rich hypernuclei ${}^A_{\Lambda}Z$ in the p shell are summarized in the last column of Table 5. We used the experimentally known g.s. binding energies of same- A normal hypernuclei ${}^A_{\Lambda}Z'$ with $Z' > Z$ from [2], averaging statistically when necessary. The BMF contributions $\Delta B_{\Lambda}^{\text{g.s.}}$ (normal) to the binding energies of the ${}^A_{\Lambda}Z'$ ‘normal’ hypernuclei, taken from [10], are listed in column 4 and the BMF contributions $\Delta B_{\Lambda}^{\text{g.s.}}$ (n -rich) to the binding energies of the ${}^A_{\Lambda}Z$ neutron-rich hypernuclei value, which are reproduced in the last column of Table 4, are listed here in column 5. Finally, the predicted binding energies $B_{\Lambda}^{\text{g.s.}}$ (n -rich) of the neutron-rich hypernuclei ${}^A_{\Lambda}Z$ are listed in the last column of Table 5, were evaluated according to

$$B_{\Lambda}^{\text{g.s.}}({}^A_{\Lambda}Z) = B_{\Lambda}^{\text{g.s.}}({}^A_{\Lambda}Z') - \Delta B_{\Lambda}^{\text{g.s.}}({}^A_{\Lambda}Z') + \Delta B_{\Lambda}^{\text{g.s.}}({}^A_{\Lambda}Z). \quad (7)$$

The resulting binding energies are lower by about 0.1 MeV than those of the corresponding normal hypernuclei, except for ${}^9_\Lambda\text{Li}$ with binding energy about 0.5 MeV *larger* than that of ${}^{10}_\Lambda\text{Be}$ – ${}^{10}_\Lambda\text{B}$.

The relatively small effects induced by the $\Lambda\Sigma$ coupling interaction on $B_\Lambda^{\text{g.s.}}$ persist also in the particle-stable portion of neutron-rich Λ hypernuclear spectra. Here we only mention that, except for ${}^{12}_\Lambda\text{Be}$, one anticipates a clear separation about or exceeding 3 MeV between g.s. (in ${}^9_\Lambda\text{He}$) or g.s.-doublet (in ${}^{10}_\Lambda\text{Li}$ and ${}^{14}_\Lambda\text{B}$) and the first-excited hypernuclear doublet. Thus, the g.s. or its doublet are likely to be observed in experimental searches of neutron-rich Λ hypernuclei using ${}^9\text{Be}$, ${}^{10}\text{B}$, and ${}^{14}\text{N}$ targets, provided a resolution of better than 2 MeV can be reached.

4.2. Medium weight and heavy hypernuclei

It was demonstrated in the previous subsection that the $\Lambda\Sigma$ coupling contributions to p -shell hypernuclear binding energies are considerably smaller than for the s -shell $A = 4$ hypernuclei. The underlying $\Lambda\Sigma$ matrix elements decrease by roughly factor of two upon going from the s shell to the p shell, and the resulting energy contributions roughly by factor of four. This trend persists upon going to heavier hypernuclei and, as shown below, it more than compensates for the larger $N - Z$ neutron excess available in heavier hypernuclei. To demonstrate how it works, we outline schematic shell-model weak-coupling calculations using G -matrix $\Lambda\Sigma$ central interactions generated from the NSC97f YN potential model by Halderson [25], with input and results listed in Table 6 across the periodic table. We note that although the separate contributions $\Lambda\Sigma(\bar{V})$ and $\Lambda\Sigma(\Delta)$ in ${}^9_\Lambda\text{He}$ differ from those using the Akaishi interaction (see Table 4), the summed $\Lambda\Sigma$ contribution is the same to within 2%. For ${}^{49}_\Lambda\text{Ca}$, its ${}^{48}\text{Ca}$ core consists of $0s, 0p, 1s - 0d$ closed shells of protons and neutrons, plus a closed $0f_{7/2}$ neutron shell with isospin $T = 4$. The required $0f_N 0s_\Lambda \leftrightarrow 0f_N 0s_\Sigma$ radial integrals are computed for HO $n\ell_N$ radial wavefunctions with $\hbar\omega = 45A^{-1/3} - 25A^{-2/3}$ MeV and are compared in the table to the $0p_N 0s_\Lambda \leftrightarrow 0p_N 0s_\Sigma$ radial integrals for ${}^9_\Lambda\text{He}$. The decrease in the values of $\bar{V}_{\Lambda\Sigma}$ and of $\Delta_{\Lambda\Sigma}$ upon going from ${}^9_\Lambda\text{He}$ to ${}^{49}_\Lambda\text{Ca}$ is remarkable, reflecting the poorer overlap between the hyperon $0s_Y$ and the nucleon $0\ell_N$ radial wavefunctions as ℓ_N increases. The resulting $\Lambda\Sigma$ contributions to the binding energy are given separately for the Fermi spin-independent interaction using the listed values of $\bar{V}_{\Lambda\Sigma}$, and for the GT spin-dependent interaction using the listed values of $\Delta_{\Lambda\Sigma}$. The Fermi contribution involves a

$0^+ \rightarrow 0^+$ core transition preserving the value of T , see Eq. (2). The GT contribution consists of three separate $0^+ \rightarrow 1^+$ core transitions of comparable strengths, transforming a $f_{7/2}$ neutron to (i) $f_{7/2}$ nucleon with nuclear-core isospin $T_N = 3$, or to $f_{5/2}$ nucleon with (ii) $T_N = 3$ or (iii) $T_N = 4$. The overall $\Lambda\Sigma$ contribution of 24 keV in ${}^{49}_{\Lambda}\text{Ca}$ is rather weak, one order of magnitude smaller than in ${}^9_{\Lambda}\text{He}$.

Table 6: $\Lambda\Sigma$ matrix elements and contributions to binding energies (in MeV) for neutron-rich hypernuclei across the periodic table, using NSC97f YN interactions from Halderson [25]. In all cases, the diagonal matrix element is given by $\sqrt{(T+1)/3T} \sum (2j+1) \bar{V}_{\Lambda\Sigma}^{n\ell_N}$, where the sum runs over orbits in the neutron excess.

$N-Z$	${}^A_{\Lambda}Z$	$\bar{V}_{\Lambda\Sigma}$	$\Lambda\Sigma(\bar{V})$	$\Delta_{\Lambda\Sigma}$	$\Lambda\Sigma(\Delta)$	$\Delta B_{\Lambda}^{\text{g.s.}}(\Lambda\Sigma)$
4	${}^9_{\Lambda}\text{He}$	1.194	0.143	4.070	0.104	0.246
8	${}^{49}_{\Lambda}\text{Ca}$	0.175	0.010	0.946	0.014	0.024
22	${}^{209}_{\Lambda}\text{Pb}$	0.0788	0.052	0.132	0.001	0.053

In ${}^{209}_{\Lambda}\text{Pb}$, the 44 excess neutrons run over the $2p$, $1f$, $0h_{9/2}$ and $0i_{13/2}$ orbits. The Fermi $0^+ \rightarrow 0^+$ core transition is calculated using Eq. (2) where, again, $\bar{V}_{\Lambda\Sigma}$ (with a value listed in Table 6) stands for the $(2j+1)$ average of the separate neutron-excess $\bar{V}_{\Lambda\Sigma}^{n\ell_N}$ radial integrals, resulting in a $\Lambda\Sigma$ contribution of merely 52 keV to the binding energy of ${}^{209}_{\Lambda}\text{Pb}$. For the calculation of the GT $0^+ \rightarrow 1^+$ core transitions, we define $\Delta_{\Lambda\Sigma}$ as a $(2j+1)$ average of $\Delta_{\Lambda\Sigma}^{n\ell_N}$ radial integrals over the neutron-excess incomplete LS shells $0h_{9/2}$ and $0i_{13/2}$ (with a value listed in the table). These are the neutron orbits that initiate the GT core transitions required in ${}^{209}_{\Lambda}\text{Pb}$, with structure similar to that encountered in ${}^{49}_{\Lambda}\text{Ca}$ for the $0f_{7/2}$ neutron orbit; details will be given elsewhere, suffice to say here that neither of these transitions results in a $\Lambda\Sigma$ contribution larger than 0.2 keV to the binding energy of ${}^{209}_{\Lambda}\text{Pb}$.

5. Summary and outlook

In this Letter we have presented detailed shell-model calculations of p -shell neutron-rich Λ hypernuclei using (i) ΛN effective interactions derived by fitting to comprehensive γ -ray hypernuclear data, and (ii) theoretically motivated $\Lambda\Sigma$ interaction terms. None of the large effects conjectured by Akaishi and Yamazaki [5] to arise from $\Lambda\Sigma$ coherent coupling in neutron-rich

hypernuclei is borne out by these realistic shell-model calculations. This is evident from the relatively modest $\Lambda\Sigma$ component of the total BMF contribution to the Λ hypernuclear g.s. binding-energy, marked $\Delta B_{\Lambda}^{\text{g.s.}}$ in Table 4. It should be emphasized, however, that $\Lambda\Sigma$ coupling plays an important role in doublet spacings in p -shell hypernuclei [10], just as it does for ${}^4_{\Lambda}\text{H}$ and ${}^4_{\Lambda}\text{He}$ [6]. Although the ground-state doublet spacings in ${}^{10}_{\Lambda}\text{Li}$ and ${}^{14}_{\Lambda}\text{B}$ probably can't be measured, $\Lambda\Sigma$ coupling contributes 40% and 55% to the predicted doublet spacings of 341 and 173 keV, respectively (similar relative strengths as for ${}^{16}_{\Lambda}\text{O}$ [10]; the ${}^{12}_{\Lambda}\text{Be}$ doublet spacing, however, is predicted to be very small). Forthcoming experiments searching for neutron-rich Λ hypernuclei at J-PARC will shed more light on the $N - Z$ dependence of hypernuclear binding energies.

We have also discussed in detail the shell-model argumentation for a slightly particle-stable ${}^6_{\Lambda}\text{H}$, comparing it with predictions by Akaishi et al. that overbind ${}^6_{\Lambda}\text{H}$ as well as with a very recent four-body calculation by Hiyama et al. that finds it particle-unstable. In the former case [5, 19], we have argued that the effects of $\Lambda\Sigma$ coupling in ${}^6_{\Lambda}\text{H}$ cannot be very much larger than they are in ${}^4_{\Lambda}\text{H}$, whereas such effects are missing in the latter case [23]. Genuine YNN three-body contributions are missing so far in *all* calculations of ${}^6_{\Lambda}\text{H}$, and need to be implemented. Systematic studies of these contributions, which appear first at NNLO EFT expansions, have not been made to date in hypernuclear physics where the state of the art is just moving from LO to NLO applications [26]. At present, and given the regularity of hypernuclear binding energies of heavy Λ hypernuclei with respect to those in light and medium-weight hypernuclei as manifest in SHF-motivated density-dependent calculations [27], in RMF [28] and in-medium chiral SU(3) dynamics calculations [29] extending over the whole periodic table, no strong phenomenological motivation exists to argue for substantial $N - Z$ effects in Λ hypernuclei. Indeed, this was demonstrated in the calculation outlined in the previous section for ${}^{49}_{\Lambda}\text{Ca}$ and ${}^{209}_{\Lambda}\text{Pb}$.

Acknowledgements

We thank Emiko Hiyama and Jiří Mareš for useful comments made on a previous version of this work. D.J.M. acknowledges the support by the U.S. DOE under Contract DE-AC02-98CH10886 with the Brookhaven National Laboratory, and A.G. acknowledges support by the EU initiative FP7, HadronPhysics3, under the SPHERE and LEANNIS cooperation programs.

References

- [1] R.H. Dalitz, R. Levi Setti, *Nuovo Cimento* 30 (1963) 489; see also L. Maffling, *Nucl. Phys. A* 585 (1995) 211c.
- [2] D.H. Davis, *Nucl. Phys. A* 754 (2005) 3c, and references listed therein, particularly D.H. Davis, J. Pniewski, *Contemp. Phys.* 27 (1986) 91.
- [3] M. Agnello, et al. (FINUDA Collaboration and A. Gal), *Phys. Rev. Lett.* 108 (2012) 042501.
- [4] M. Agnello, et al. (FINUDA Collaboration and A. Gal), *Nucl. Phys. A* 881 (2012) 269.
- [5] Y. Akaishi, T. Yamazaki, in *Physics and Detectors for DAΦNE*, Eds. S. Bianco et al., Frascati Physics Series Vol. XVI (INFN, Frascati, 1999) pp. 59-74.
- [6] Y. Akaishi, T. Harada, S. Shinmura, K.S. Myint, *Phys. Rev. Lett.* 84 (2000) 3539.
- [7] H. Nemura, Y. Akaishi, Y. Suzuki, *Phys. Rev. Lett.* 89 (2002) 142504.
- [8] S. Shinmura, K.S. Myint, T. Harada, Y. Akaishi, *J. Phys. G* 28 (2002) L1, and a revised calculation by S. Shinmura, et al., *Mod. Phys. Lett. A* 18 (2003) 128.
- [9] T. Takahashi, *Nucl. Phys. A* (HYP2012 Proceedings, in press) <http://dx.doi.org/10.1016/j.nuclphysa.2012.12.118>, and J-PARC E10, http://j-parc.jp/researcher/Hadron/en/Proposal_e.html.
- [10] D.J. Millener, *Nucl. Phys. A* 881 (2012) 298, and references therein.
- [11] H. Tamura, et al., *Nucl. Phys. A* 835 (2010) 3, and references therein.
- [12] A. Gal, J.M. Soper, R.H. Dalitz, *Ann. Phys. (N.Y.)* 63 (1971) 53.
- [13] D.J. Millener, *Nucl. Phys. A* 835 (2010) 11.
- [14] Th.A. Rijken, V.J.G. Stoks, Y. Yamamoto, *Phys. Rev. C* 59 (1999) 21.
- [15] A. Umeya, T. Harada, *Phys. Rev. C* 83 (2011) 034310.

- [16] A. Gal, J.M. Soper, R.H. Dalitz, *Ann. Phys. (N.Y.)* 113 (1978) 79.
- [17] D.J. Millener, A. Gal, C.B. Dover, R.H. Dalitz, *Phys. Rev. C* 31 (1985) 499.
- [18] H. Tamura, et al., *Nucl. Phys. A* 881 (2012) 310, and references therein.
- [19] K.S. Myint, Y. Akaishi, *Prog. Theor. Phys. Suppl.* 146 (2002) 599; Y. Akaishi, K.S. Myint, *AIP Conf. Proc.* 1011 (2008) 277; Y. Akaishi, *Prog. Theor. Phys. Suppl.* 186 (2010) 378; Theingi, K.S. Myint, Y. Akaishi, *Genshikaku Kenkyu* 57, *Suppl.* 3 (2013) 70.
- [20] A.A. Korshennikov, et al., *Phys. Rev. Lett.* 87 (2001) 092501.
- [21] S.N. Nakamura, et al. (JLab E01-011), *Phys. Rev. Lett.* 110 (2013) 012502.
- [22] E. Hiyama, Y. Yamamoto, T. Motoba, M. Kamimura, *Phys. Rev. C* 80 (2009) 054321.
- [23] E. Hiyama, S. Ohnishi, M. Kamimura, Y. Yamamoto, *Nucl. Phys. A* 908 (2013) 29.
- [24] A. Umeya, T. Harada, *Phys. Rev. C* 79 (2009) 024315.
- [25] D. Halderson, private communication.
- [26] J. Haidenbauer, S. Petschauer, N. Kaiser, U.-G. Meißner, A. Nogga, W. Weise, *Nucl. Phys. A* 915 (2013) 24.
- [27] D.J. Millener, C.B. Dover, A. Gal, *Phys. Rev. C* 38 (1988) 2700.
- [28] J. Mareš, B.K. Jennings, *Phys. Rev. C* 49 (1994) 2472.
- [29] P. Finelli, N. Kaiser, D. Vretenar, W. Weise, *Nucl. Phys. A* 831 (2009) 163.